Fully Lagrangian Approach of Three-Phase Systems for Debris Bed Formation (Part IV: Self-generated bubble condition)

YoungWoo Son, InSoo Seo, Cheol-O Ahn*
Metariver Technology Co., Ltd., C-716, Moonjeong-SK-V1, 128, Beobwon-ro, Songpa-gu, Seoul, 05854, Republic of Korea
**Corresponding author: coahn@metariver.kr*

Keywords : DAVINCI experiment, three-phase flow, Discrete Bubble Model (DBM), Moving Particle Semi-implicit (MPS), Discrete Element Method (DEM)

1. Introduction

In a severe LWR (Light-Water Reactor) accident involving core fuel melting, corium released outside the reactor is expected to form a porous debris layer that accumulates at the bottom of the pool. To evaluate the coolability of this corium debris layer, understanding its formation process and geometric shape is essential.

Kim et al. [1][2] investigated the external shape of a debris bed affected by two-phase flow induced by vapor generation from the decay heat of the debris layer using the DAVINCI facility. In this experiment, they injected 5 kg of stainless-steel simulant particles, each with a diameter and height of 2 mm, from the top of the water surface. (The equivalent volume diameter of the particle is 2.29. (D_V2.29)) They injected air bubbles simulating vapor flow from the bottom of the particle catcher plate. The airflow rate was determined based on the amount of settled debris, which will form a heat source due to the decay of corium. The radial distribution of the settled debris was analyzed using a five-step "gap-tooth" approach. The method they employed used the particle layer generated in the previous step as the initial conditions for the next step, with each step designed to drop 1 kg of simulated particles for approximately 10 seconds. Therefore, the experiment, consisting of five stages, allowed for the observation of particle layer formation at each stage by dropping 5 kg of simulated particles over 50 seconds.

In Part 1 of the paper with the same title [3], simulation results using a coupled MPS-DEM-DBM approach based on a fully Lagrangian method were compared quantitatively with DAVINCI experiments (internal structure). Part 2 [4] involved simulations were conducted to examine the mass distribution of particles settling on the bottom, based on particle sphericity. Part 3 compared simulation results with DAVINCI experiments (external shape). Finally, Part 4 included conditions for self-generated bubbles from debris, rather than from air-injected bubble columns.

To distinguish this condition from the TPC in the DAVINCI experiments, this paper refers to it as SGC (Self-generated Bubble Conditions from debris). The interaction between the particle column created by falling particles and the bubble column generated by decay heat results in collisions and complex behaviors that lead to particle dispersion to the bottom. While bubbles produced by air injection and those formed in self-generated bubble columns from debris are expected to share similar formation mechanisms, simulations were conducted to explore how these differences influence debris layer formation.

The external shape of the debris bed influences how the liquid volume fractions of individual particles are distributed, which in turn affects the local bubble generation rate and ultimately the dispersion of falling particles. We believe that numerical analysis under SGC conditions can better explain the interaction between bed shape and bubble generation rate.

In addition, to investigate the effect of particle size on the external shape of the debris layer, numerical analysis was performed on 3 mm and 5 mm particles of the same shape with the same diameter and height under the same conditions. (D_V3.43 and D_V5.72)

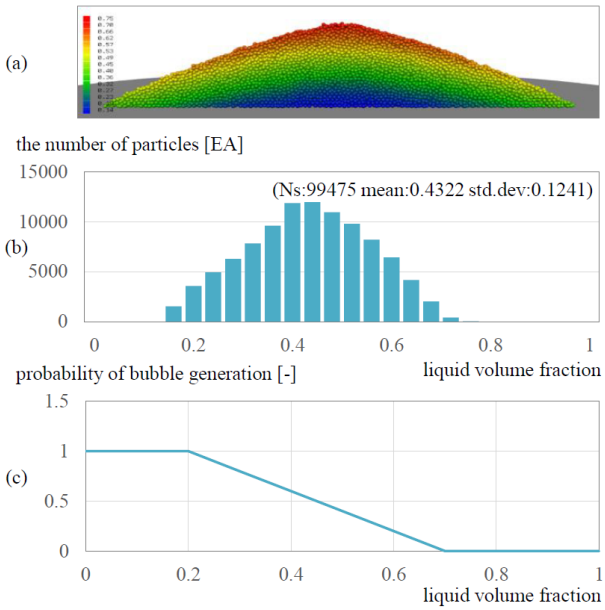

Fig. 1. Conditions for generating bubbles from the debris
(a) liquid volume fraction (QPC5, cross-section view)
(b) the histogram of the liquid volume fraction
(c) probability function for bubble generation

2. DAVINCI experiment

According to KIM et al., the following assumptions were made in this experiment: First, the water depth was sufficiently deep, and the melt jet diameter was relatively small, which allowed for complete fragmentation of the corium melt jet. Second, vapor generation due to phase change within the debris layer was estimated based on volumetric decay heat, assuming that the decay heat of the corium particles was the only source. In other words, natural convection due to decay heat was not considered. Third, particle remelting was not taken into account. Finally, although bubbles can flatten the existing debris layer over a relatively long period, self-leveling was ignored. [1][2]

For more details on the DAVINCI experiment, see Part III of the paper with the same title.

3. Numerical method

We implemented the MPS method proposed by Koshizuka et al. for analysing the continuous phase. MPS [5] uses a semi-implicit algorithm to calculate the pressure field by solving the Poisson Pressure Equation (PPE), ensuring incompressibility and stability of the fluid. To account for turbulence, we incorporated the Subgrid-scale turbulence model for Large-eddy simulation of MPS introduced by Gotoh et al., the wall model proposed by Arai et al., and the Contoured Continuum Surface Force model by Duan et al. to compute surface tension forces.

The Discrete Element Method (DEM) was used to analyze the behavior of solid particles. In DEM, a nonlinear viscoelastic model based on the Hertz-Mindlin contact force model is used to calculate collisions between particles and between particles and walls. Di Feice's correlation was used to consider the swarm effect of particles on the drag coefficient. Additionally, the Haider and Levenspiel correlations were used to account for the drag of non-spherical particles. To account for particle lift, we used the correlation proposed by Shi and Rzehak, and adopted the method proposed by Sato et al. for the particle/bubble-induced turbulence model. The total viscosity of the liquid was calculated as the sum of molecular viscosity, eddy viscosity due to turbulence, and viscosity induced by particles and bubbles.

To analyze bubble behavior, the Discrete Bubble Method (DBM) based on the Lagrangian approach was used, as first introduced by Delnoij et al. [6]. The movement of each bubble is determined by considering external forces such as gravity, pressure gradient, drag, lift, and virtual mass. In this study, the Tomiyama model (for slightly contaminated systems) was adopted to calculate the drag coefficient, and the Rouche model, which accounts for interaction effects between adjacent bubbles, was used. Tomiyama's lift coefficient correlation was employed to account for the lift force acting perpendicular to the relative motion between the bubble and the fluid. To account for particle lift, we used the correlation proposed by Shi and Rzehak, and adopted the method proposed by Sato et al. for the particle/bubble-induced turbulence model.

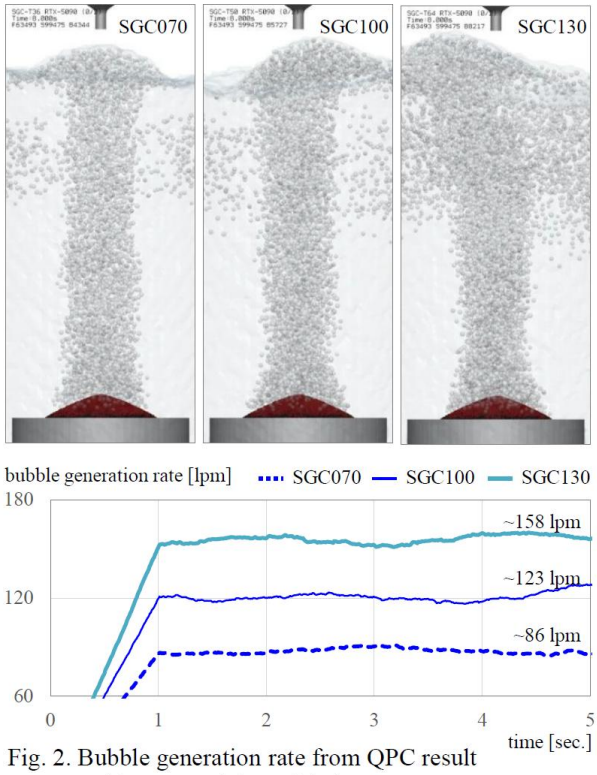

Fig. 2. Bubble generation rate from QPC result (self-generated from debris, D_V2.92)

In this study, for accurate volume fraction calculation using the gridless particle-based method, the approach of directly calculating the volume defined by the overlap between the virtual sphere, defined by the coupling radius, and an arbitrary sphere was used. [7]

For more details on the numerical method, see Part III of the paper with the same title.

4. Numerical analysis

Fig. 1 shows the conditions for self-generated bubbles from debris. First, the liquid volume fraction of particles was analyzed using the QPC5 results and displayed as a histogram in Fig. 1(b). Particles with a high liquid volume fraction in the debris bed are less likely to generate vapor through phase change, as they transfer heat more actively to the fluid than particles with a low liquid volume fraction. Conversely, particles with a low liquid volume fraction are more likely to actively generate vapor. Therefore, as shown in Fig. 1(c), a probability function based on the liquid volume fraction was employed to ensure vapor generation occurs according to this fraction. The external shape of the debris bed affects the distribution of the liquid volume fraction of individual particles.

Fig. 2 illustrates the simulation results for the bubble generation rate per unit time in the debris bed, derived

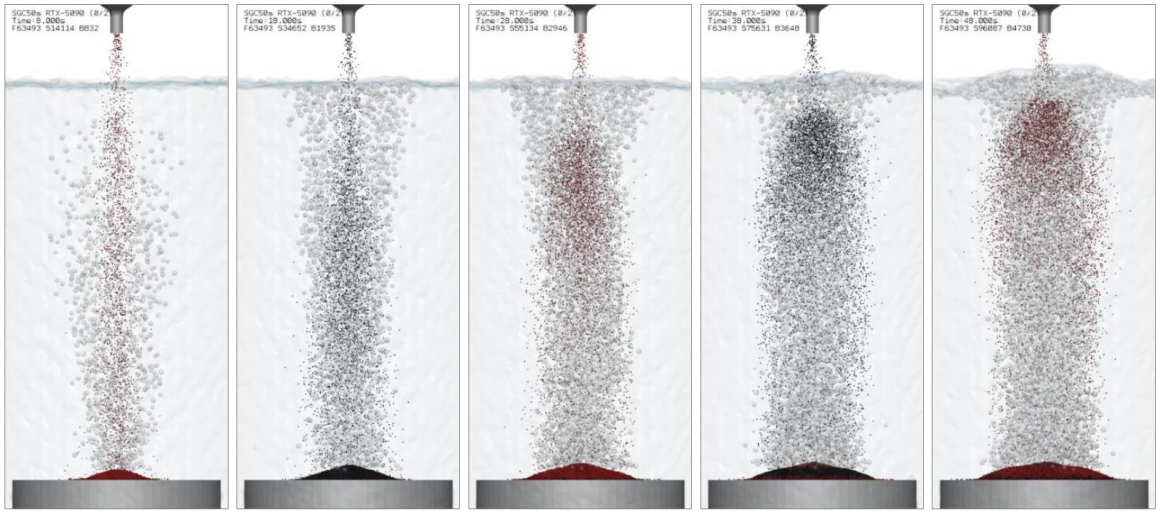

(a) 8 sec. (b) 18 sec. (c) 28 sec. (d) 38 sec. (e) 48 sec.

Fig. 3. Snapshots at 10-second intervals during simulation (D_V2.92, SGC100, sphericity 0.874)

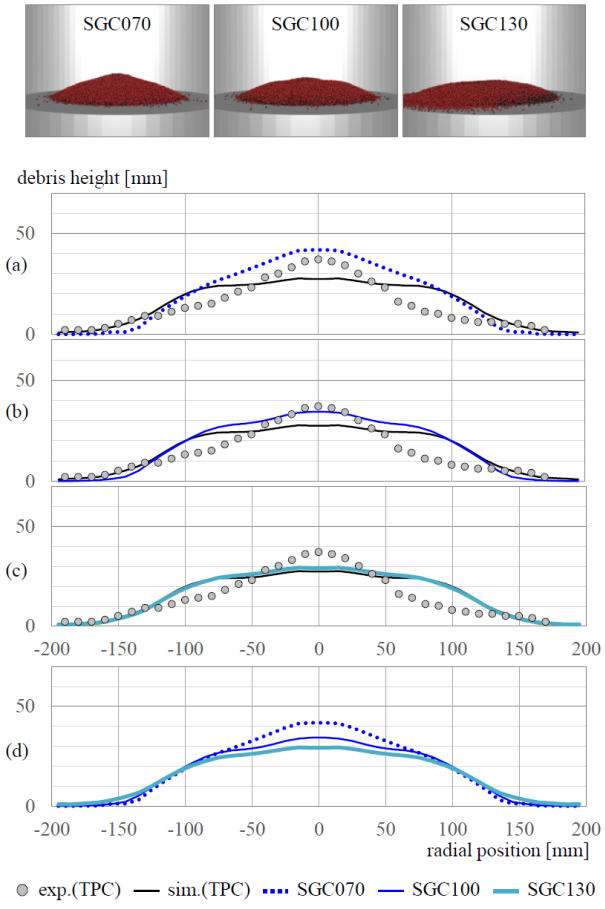

Fig. 4. Comparison of the debris bed according to the bubble generation rate (D_V2.92, sphericity 0.874)
(a) SGC070 (b) SGC100 (c) SGC130
(d) SGC070, SGC100, and SGC130

from the QPC5 results and based on the previously established conditions. At regular time intervals, the liquid volume fraction of the particles examined was applied to the probability function in Fig. 1 (c) to generate bubbles. Using the TPC5 conditions (120.8 lpm), the bubble generation rate was set to three levels: 70%, 100%, and 130%. These are labelled as SGC070, SGC100, and SGC130.

As in Part 3 of this paper, bubbles with a diameter between 8 mm and 12 mm were generated in the simulation, and two particle sphericities of 0.874 and 1.0 were used.

Additionally, to examine the effect of particle size on the external shape of the debris bed, numerical analysis was performed for particles with a diameter and height of 3 mm and for particles with a diameter and the same diameter-height of 5 mm under the same conditions as above (four bubble generation rate conditions, including QPC and two sphericity conditions). When expressed as equivalent volume diameters, these are expressed as D_V3.43 and D_V5.72, respectively.

5. Results

Fig. 3 displays five snapshots taken every 10 seconds from a simulation of dropping 5 kg of particles with a sphericity of 0.874 over 50 seconds under SGC100 conditions.

Fig. 4 compares the results of three simulations using particles with a sphericity of 0.874 with the TPC experiment. These graphs display the average bed height in the circumferential direction. The simulation results under SGC100 conditions closely match the TPC experiment by KIM et al., and the results are nearly identical to the TPC analysis results (TPC5) obtained using the five-step gap-tooth method. As shown in Fig. 4(d), as the bubble generation rate increases, the maximum height of the debris bed slightly decreases, while the radial growth remains very small.

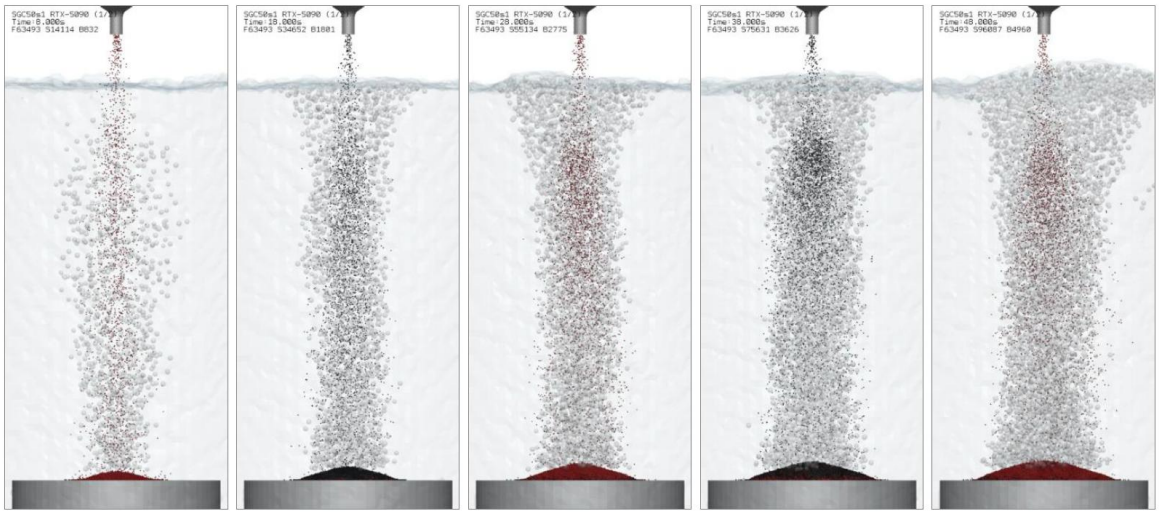

(a) 8 sec. (b) 18 sec. (c) 28 sec. (d) 38 sec. (e) 48 sec.

Fig. 5. Snapshots at 10-second intervals during simulation (D_V2.92, SGC100, sphericity 1.0)

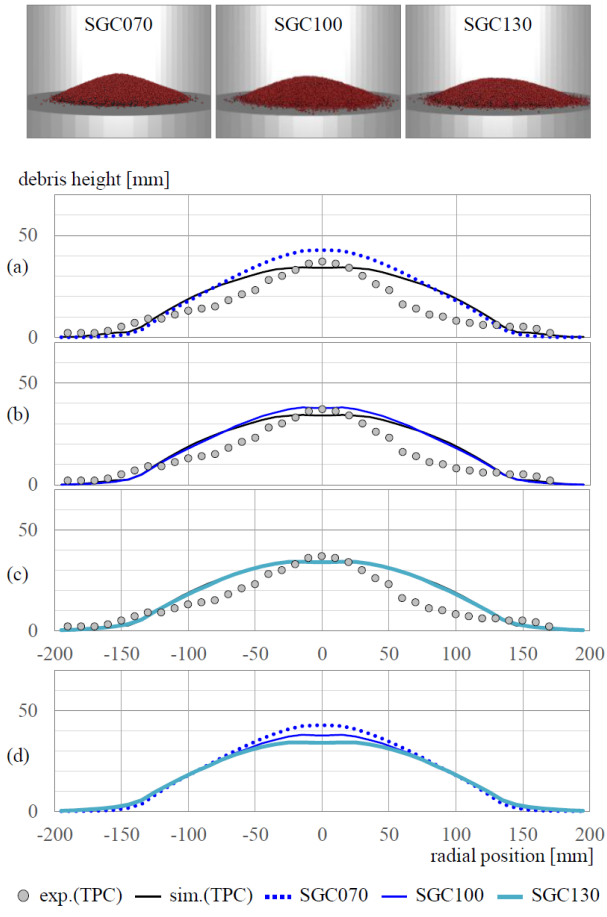

Fig. 6. Comparison of the debris bed according to the bubble generation rate (D_V2.92, sphericity 1.0)
(a) SGC070 (b) SGC100 (c) SGC130
(d) SGC070, SGC100, and SGC130

Fig. 5 shows five snapshots taken at 10-second intervals from a simulation of dropping 5 kg of particles with a sphericity of 1.0 over 50 seconds under SGC100 conditions. Fig. 6 compares the results of three simulations using particles with a sphericity of 1.0 with the TPC experiment. Similar to the previous sphericity of 0.874, the simulation results obtained under SGC100 conditions were most consistent with the TPC experiment, and the results were nearly identical to the TPC analysis results (TPC5) using the five-step gap-tooth method. As shown in Fig. 6(d), as the bubble generation rate increased, the maximum height of the debris bed slightly decreased, but radial growth remained minimal.

For comparison based on sphericity, snapshots taken at the same time under the SGC100 condition are shown in Fig. 7, and those under the SGC130 condition are shown in Fig. 8. As sphericity increases, particles exhibit a lower drag coefficient and become less affected by the upward flow induced by the bubble column. Consequently, the radial dispersion of particles decreases with increasing sphericity, causing them to settle more in the central region of the PCP. This can be more easily explained with Fig. 9 and 10. KIM et al. used the radius of a circle containing 75% of the particle volume as a scale to describe radial dispersion, denoted as R75. Fig. 9 compares the maximum height of the debris bed obtained under each condition, and Fig. 10 compares the R75. As the bubble generation rate increased, the maximum height of the debris bed decreased approximately linearly, while R75 increased slightly.

Compared to the TPC simulation using the five-step gap-tooth method, the maximum bed height was measured lower for the SGC100 condition with a sphericity of 0.874, while it was estimated to be similar for the sphericity of 1.0.

Fig. 11 compares the bubble generation rate over time obtained from simulations under two sphericity conditions and three bubble generation rate conditions. As previously noted, the external shape of the debris bed may affect the liquid volume fraction of individual

(a) D_V2.92, sphericity 0.874 (b) D_V2.92, sphericity 1.0

Fig. 7. Snapshot comparison of SGC100 at 38 seconds. (D_V2.92)

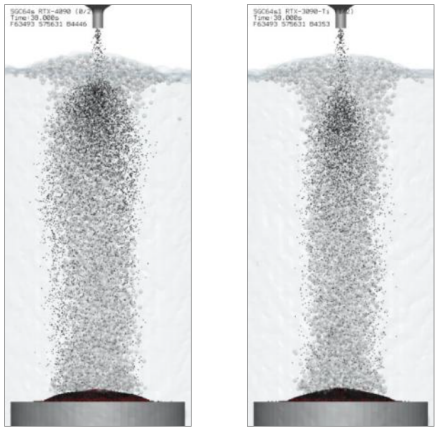

(a) D_V2.92, sphericity 0.874 (b) D_V2.92, sphericity 1.0

Fig. 8. Snapshot comparison of SGC130 at 38 seconds. (D_V2.92)

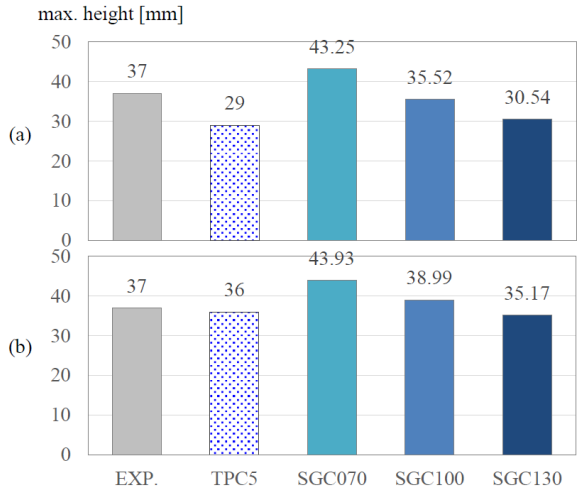

Fig. 9. Comparison of the max. height of the bed (D_V2.92) (a) sphericity 0.874 (b) sphericity 1.0

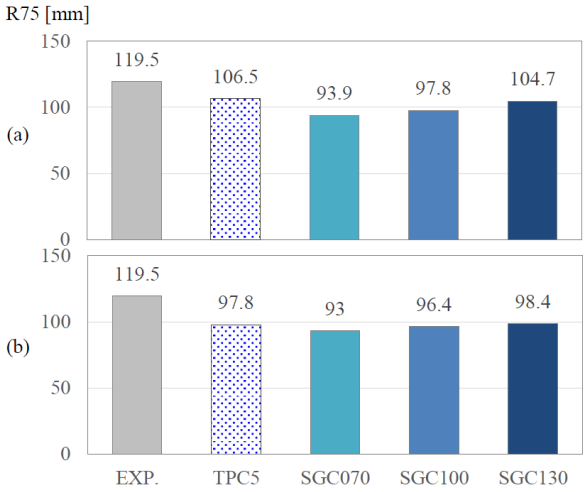

Fig. 10. Comparison of the R75 (D_V2.92) (a) sphericity 0.874 (b) sphericity 1.0

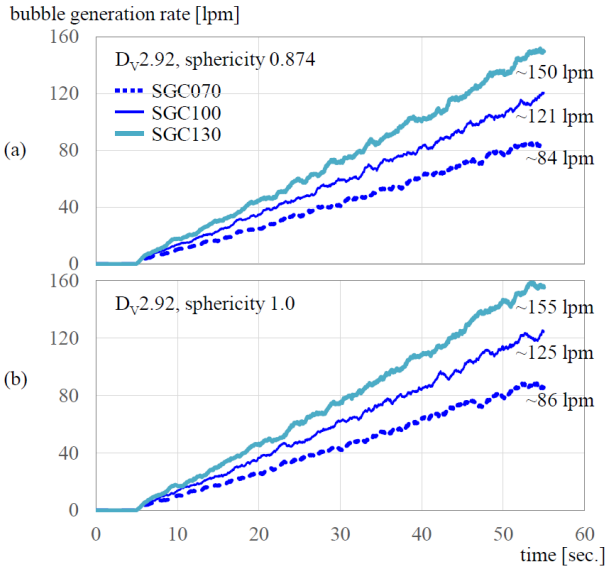

Fig. 11. Bubble generation rate obtained from SGC simulations (D_V2.92) (a) sphericity 0.874 (b) sphericity 1.0

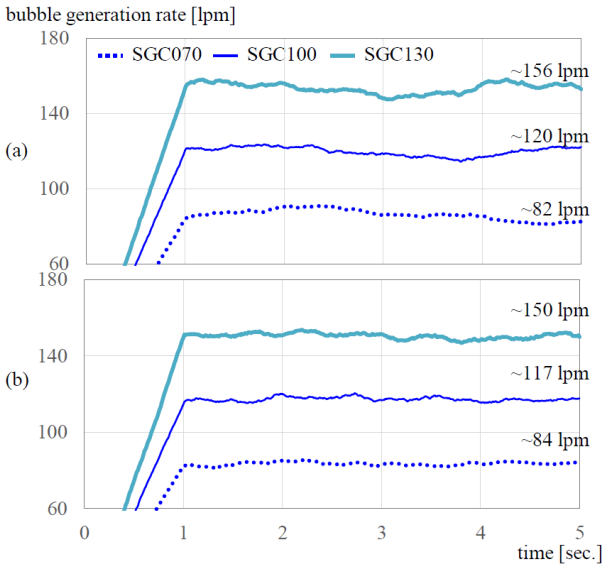

Fig. 12. Bubble generation rate from QPC result (self-generated from debris) (a) D_V3.43 (b) D_V5.72

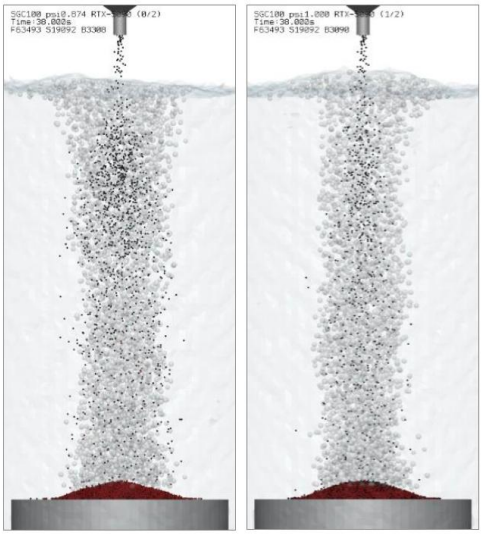

(a) D_V3.43, sphericity 0.874 (b) D_V3.43, sphericity 1.0

Fig. 13. Snapshot comparison of SGC100 at 38 seconds. (D_v3.43)

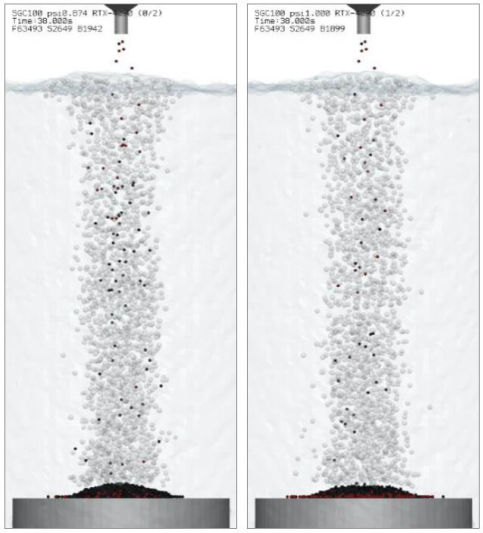

(a) D_V5.72, sphericity 0.874 (b) D_V5.72, sphericity 1.0

Fig. 14. Snapshot comparison of SGC100 at 38 seconds. (D_v5.72)

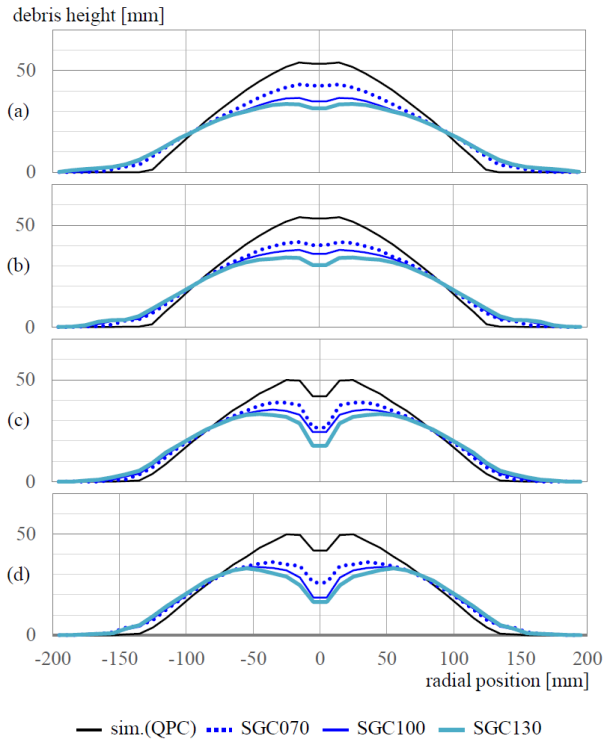

Fig. 15. Comparison of the debris bed according to the bubble generation rate
(a) D_V3.43 sphericity 0.874
(b) D_V3.43 sphericity 1.0
(c) D_V5.72 sphericity 0.874
(d) D_V5.72 sphericity 1.0

particles and, in turn, the bubble generation rate. However, compared to the bubble generation rate obtained from the QPC5 results (Fig. 2), the six simulations, despite having similar but different bed shapes, yielded identical final results. Therefore, under these conditions, it can be said that the effect of the external shape of the debris bed on the bubble generation rate was negligible.

To examine the effect of particle size on the external shape of the debris bed, numerical analysis was conducted on particles with the equivalent volume diameter of 3.43 (D_V3.43) and 5.72 (D_V5.72), respectively, under the same conditions as above (four bubble generation rate conditions, including QPC and two sphericity conditions). Fig. 12 shows the bubble generation rate under SGC conditions, where bubbles are generated from the debris bed obtained by dropping 5 kg of particles under bubble-free QPC conditions. As with the previous analysis, three conditions corresponding to 70%, 100%, and 130% were set based on the final air injection volume (120.8 lpm) of the DAVINCI experiment.

Fig. 13 and 14 show the results of numerical analysis performed on D_V3.43 and D_V5.72 particles under the SGC100 condition. As sphericity increased, the particles became slightly more concentrated toward the center due to lower drag.

Fig. 15 compares the height of the debris bed obtained under four bubble generation rate conditions, including two sphericity conditions and QPC conditions, for two particles. A central dimple, which did not occur in the case of D_V2.92, appeared small in the case of D_V3.43 and was clearly observed in the center in the case of D_V5.72.

Fig. 16 compares the maximum height of the debris bed obtained under each condition, and Fig. 17 compares R75, which was used as a measure to explain the radial dispersion of particles. As the bubble generation rate increased, the maximum height of the debris bed decreased, and R75 increased slightly.

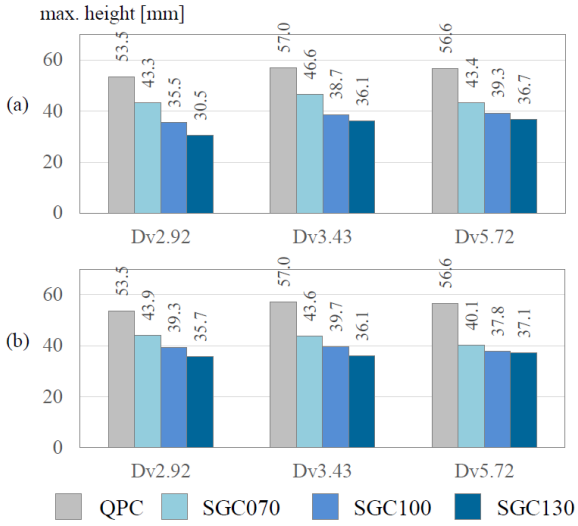

Fig. 16. Comparison of the max. height of the bed
(a) sphericity 0.874 (b) sphericity 1.0

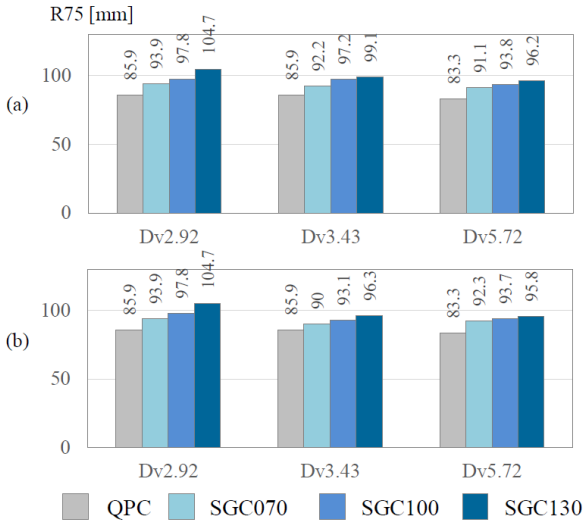

Fig. 17. Comparison of the R75
(a) sphericity 0.874 (b) sphericity 1.0

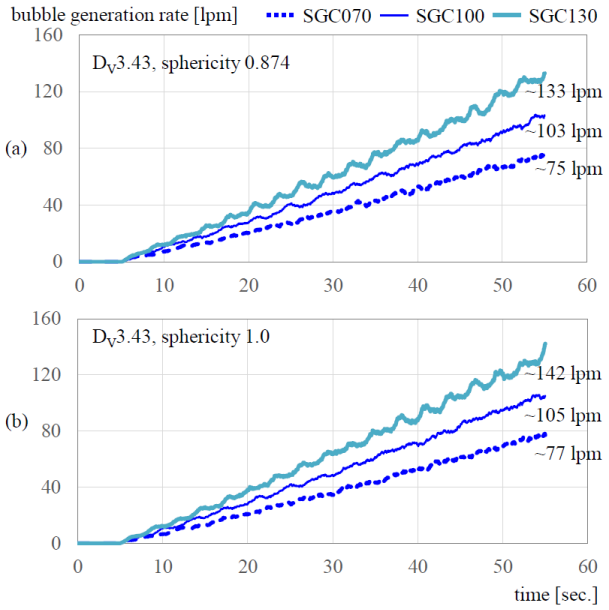

Fig. 18. Bubble generation rate obtained from SGC simulations (D_V3.43)
(a) sphericity 0.874 (b) sphericity 1.0

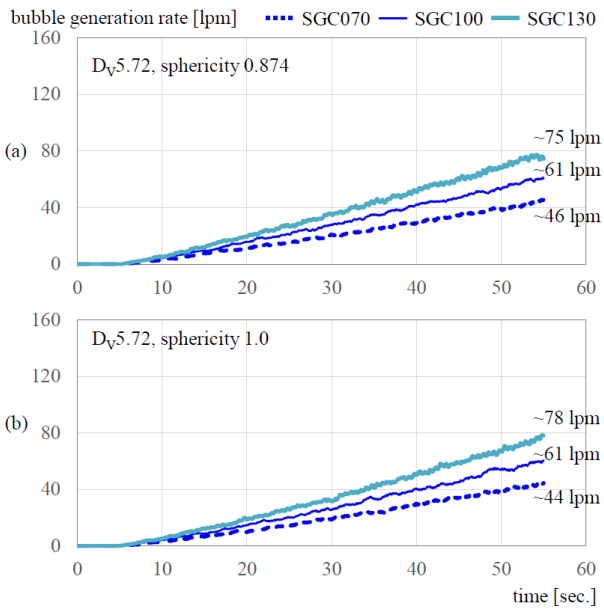

Fig. 19. Bubble generation rate obtained from SGC simulations (D_V5.72)
(a) sphericity 0.874 (b) sphericity 1.0

The external shape of the debris bed affects the distribution of liquid volume fractions within individual particles, which, in turn, influences the local bubble generation rate and ultimately the dispersion of falling particles. By comparing Fig. 2 and Fig. 11, it was found that the effect of the external shape of the debris bed on the bubble generation rate was negligible in the case of D_V2.92; however, through a comparison of Fig. 12, 18, and 19, it was found that the effect became significant as the particle size increased. This suggests that the difference in the shape of the debris bed obtained under QPC and SGC conditions significantly affected the liquid volume fraction. It is thought that the particle size condition, as well as the shape of the dimples observed in Fig. 15, played a significant role in this result.

6. Conclusions

In this study, we used an unresolved method to combine MPS, DEM, and DBM in a fully Lagrangian approach to simulate the collision of a particle column formed by falling debris particles with self-generated bubbles from settled debris particles.

Comparison with the TPC results using the five-step gap-tooth method yields results similar to those obtained under self-generated bubble conditions from settled debris particles (SGC). Under SGC conditions

with an equivalent volume diameter of 2.92, the maximum bed height was measured to be lower for the SGC100 condition with a sphericity of 0.874 compared to the TPC condition, while it was evaluated to be similar for a sphericity of 1.0. Although significant uncertainty exists due to the complex movement of many bubbles and particles caused by numerous collisions and the resulting fluid flow, consistent and valid trends were confirmed from simulation results varying particle sphericity and bubble generation rates.

The external shape of the debris bed affects the distribution of liquid volume fractions of individual particles, which in turn influences the local bubble generation rate and ultimately affects the dispersion of falling particles. Numerical analysis results showed that for small particles (D_V2.92), the effect of the debris bed's external shape on the bubble generation rate was negligible, but the effect became significant as the particle size increased.

The following limitations are noted in the numerical analysis.

First, coalescence and bubble breakup were not considered in this study. When a rising bubble and a falling particle collide, it is expected that a large bubble will break into smaller bubbles and that two rising bubbles will merge into one under certain conditions. However, research on this phenomenon is still limited, and although some researchers have attempted numerical analysis, no clear model has yet been established.

Second, the drag and lift forces calculated for dispersed phases, such as bubbles and particles, are steady forces, and unsteady forces are not considered. Research on these unsteady forces is also limited, and modelling or numerical implementation requires substantial memory and computational resources.

REFERENCES

[1] E. Kim, M. Lee, H. Park, K. Moriyama, and J. Park, Development of an ex-vessel corium debris bed with two-phase natural convection in a flooded cavity, Nuclear Eng. and Design, Vol. 298, pp. 240-254, 2016.

[2] E. Kim, Debris Bed Formation during Ex-Vessel Severe Accidents in Light Water Reactors, Doctoral Thesis, Pohang University of Science and Technology, 2016.

[3] Y. Son, I. Seo, and C. Ahn, Fully Lagrangian Approach of Three-Phase Systems for Debris Bed Formation (Part I: DAVINCI experiment), Trans. of the Korean Nuclear Soc. Spring Meeting, 2025.

[4] Y. Son, I. Seo, and C. Ahn, Fully Lagrangian Approach of Three-Phase Systems for Debris Bed Formation (Part II: Effect of Sphericity), Trans. of the Korean Nuclear Soc. Spring Meeting, 2025.

[5] S. Koshizuka, K. Shibata, M. Kondo, and T. Matsunaga, Moving Particle Semi-Implicit Method, Academic Press, 2018.

[6] E. Delnoij, J.A.M. Kuipers, and W. Van Swaaij, A three-dimensional CFD model for gas–liquid bubble columns. Chem. Eng. Sci., Vol. 54, pp. 2217–2226, 1999.

[7] Y. Son, C. Ahn, S. Lee, Using a Lagrangian-Lagrangian Approach for Studying Flow Behavior Inside a Bubble Column, Nuclear Eng. and Tech., Vol. 55, pp. 4395-4407, 2023.